NUMERICAL SOLUTION OF MHD FLOW OF CASSON FLUID OVER AN EXPONENTIALLY STRETCHING SHEET WITH THERMAL RADIATION

Dr. Shamasuddin Wani
*Corresponding Author:*Ph.D. (Mathematics)*
sdinwani@gmail.com

Dr. Shankar Rao Munjum

Abstract
This chapter examines the steady magnetohydrodynamic (MHD) boundary layer flow and heat transfer characteristics of a non-Newtonian Casson fluid over an exponentially stretching sheet in the presence of thermal radiation. The influence of a transverse magnetic field, modeled via the Lorentz force, and thermal radiation effects are incorporated into the energy equation. By applying similarity transformations, the governing nonlinear partial differential equations are reduced to a set of coupled ordinary differential equations, which are then solved numerically using the shooting method with a Runge-Kutta integration scheme. The effects of key parameters such as magnetic parameter, Casson parameter, Prandtl number, and radiation parameter on the velocity and temperature profiles are analyzed. The skin-friction coefficient and Nusselt number are also computed to evaluate the surface shear stress and rate of heat transfer. Results show that magnetic field and Casson parameters suppress the flow velocity, while thermal radiation enhances the thermal boundary layer thickness. These findings offer useful insights into industrial processes involving non-Newtonian MHD flows, such as polymer extrusion, metallurgy, and biofluid dynamics.

Keywords: *Magnetohydrodynamics (MHD), nanofluid, exponentially stretching sheet, boundary layer flow, thermal conductivity enhancement, Casson fluid*

1. Introduction:

The study of non-Newtonian fluid flows under magnetic fields has received substantial attention due to its applications in engineering and biomedical processes. Casson fluid, a type of non-Newtonian fluid, is often used to model fluids with yield stress such as blood, printing ink, and polymer solutions. In many practical scenarios, the stretching of a sheet at an exponentially increasing rate is relevant—particularly in the extrusion of plastic and metal sheets. Furthermore, when such processes occur at high temperatures, thermal radiation becomes a significant mode of heat transfer.

Incorporating magnetohydrodynamic (MHD) effects allows control over the flow behavior using magnetic fields, which is particularly useful in metallurgical and cooling systems. Thermal radiation, when included in the energy model, further refines the accuracy of simulations in high-temperature environments. This study investigates the combined effects of MHD and thermal radiation on Casson fluid flow over an exponentially stretching sheet, with the goal of characterizing the behavior of the velocity and temperature fields under varying parameter conditions.

Makinde and Animasaun (2016) incorporated the complex interaction of magnetic fields, nanoparticle motion, and microorganism activity. They demonstrated that the presence of nonlinear radiation significantly enhanced the thermal boundary layer thickness, while bioconvection led to increased motile microorganism density near the surface. The chemical reaction further intensified the transport process, indicating possible applications in bio-microreactor design and thermal regulation systems. **Mondal et al. (2017)** included magnetic field effects, which influenced the fluid velocity, temperature, and concentration profiles. Their findings highlighted the shear-thinning behavior of Casson fluids and emphasized the importance of slip parameters in reducing drag forces. The study's implications are particularly relevant for controlling fluid flow in engineering processes involving stretching surfaces, such as polymer extrusion. **Gharami et al. (2020)** used similarity transformations to reduce the governing PDEs and solved them using the Homotopy Analysis Method (HAM). Their results showed that increasing thermal radiation intensified heat transfer, whereas the chemical reaction rate significantly affected species concentration. The study serves as a benchmark for validating numerical algorithms and understanding radiative effects in chemical reactors. **Lavanya (2020)** underscored the role of viscoelasticity and micro-rotation in altering heat and mass transport. The Hall effect was shown to significantly modify velocity profiles, especially in electrically conducting fluids under strong magnetic influence. These findings are applicable to plasma flows, geophysical applications, and polymeric fluid systems. **Zaidi et al. (2020)** demonstrated that radiation enhances heat transfer, while couple stress fluid behavior reduces viscous drag near the walls. The research highlighted the interaction between

induced magnetic fields and thermal gradients, which is crucial in electromagnetic cooling and high-temperature systems. **Kemparaju et al. (2021)** considered melting at the surface and included Brownian motion and thermophoresis effects. Their results illustrated that the presence of melting and radiation significantly increases temperature distribution, while chemical reaction impacts nanoparticle concentration. The study provides insights into the melting dynamics of nanoparticles and their application in materials processing. **Khan et al. (2021)** developed a model accounting for convective boundary conditions and exothermic reactions. The analysis revealed that internal heat generation substantially boosts the fluid temperature, potentially leading to thermal runaway under certain conditions. This model can guide the safe design of thermal reactors and combustion systems. **Swapna et al. (2021)** focused on the non-Newtonian characteristics of Casson fluid and observed that higher Casson parameters reduce the flow resistance. Radiation and reaction parameters were found to amplify the thermal boundary layer and alter the species diffusion rate. The study is relevant in biomedical applications, particularly in blood flow and drug diffusion modeling. **Bhatti et al. (2022)** considered thermal energy storage and revealed that microorganism motility and nanoparticle interactions significantly impact flow structure and heat transfer. The inclusion of rotational motion and porous media effects adds depth to understanding flow dynamics in confined geometries, such as bio-reactors and thermal storage systems. **Sarifuddin (2022)** integrated geometrical irregularities of arteries and examined the influence of wall shear stress on mass transport. Results emphasized the impact of non-Newtonian behavior on blood flow resistance and pollutant dispersion, offering potential applications in cardiovascular diagnostics and targeted drug delivery. **Ullah et al. (2022)** revealed that the exponential heat source enhances thermal gradients, while the microorganisms' presence alters bioconvective flow patterns. These findings are useful in microfluidic and thermal bioengineering systems involving microorganisms and nanoparticles. **Bourchak et al. (2023)** studied radiative Williamson fluid flow with ferromagnetic nanoparticles, incorporating gyrotactic microorganism and bioconvection analysis. The introduction of ferromagnetic particles added magnetic control to the fluid, significantly modifying temperature and concentration fields. Gyrotactic effects intensified the upward movement of motile cells, enhancing mixing. This novel integration of bio-convection with magnetic nanoparticles has promising applications in advanced cooling systems and magneto-bio-reactors.

2. Physical Model and Assumptions:

(i) Steady, laminar, two-dimensional, incompressible Casson fluid flow.
(ii) Exponentially stretching sheet with velocity $u_w(x) = U_0 e^{ax}$, where $a > 0$.
(iii) (A uniform magnetic field B_0 is applied normal to the surface.
(iv)Thermal radiation is considered via the Rosseland approximation.
(v) Constant physical properties, except for radiative heat flux.
(vi) No viscous dissipation or heat generation considered.

3. Governing Equations: Let u, v be the velocity components in the x and y directions.

Continuity Equation:

$$\frac{\partial u}{\partial x} + \frac{\partial v}{\partial y} = 0 \qquad (1)$$

Momentum Equation (x-direction):

$$u\frac{\partial u}{\partial x} + v\frac{\partial u}{\partial y} = \nu\left(1 + \frac{1}{\beta}\right)\frac{\partial^2 u}{\partial y^2} - \frac{\sigma {B_0}^2}{\rho}u \qquad (2)$$

Energy Equation (with thermal radiation):

$$u\frac{\partial T}{\partial x} + v\frac{\partial T}{\partial y} = \alpha\frac{\partial^2 T}{\partial y^2} - \frac{1}{\rho c_p}\frac{\partial q_r}{\partial y} \qquad (3)$$

Using the Rosseland approximation:

$$q_r = -\frac{4\sigma^*}{3k^*}\frac{\partial T^4}{\partial y} \approx -\frac{16\sigma^* {T_\infty}^3}{3k^*}\frac{\partial T}{\partial y}$$

So the energy equation becomes:

$$u\frac{\partial T}{\partial x} + v\frac{\partial T}{\partial y} = \left(\alpha + \frac{16\sigma^* {T_\infty}^3}{3k^*\rho c_p}\right)\frac{\partial^2 T}{\partial y^2}$$

4. Similarity Transformations:

$$\eta = \sqrt{\frac{a}{\nu}}\, e^{\frac{ax}{2}} y, \psi = \sqrt{a\nu} e^{\frac{ax}{2}} f(\eta) \qquad (5)$$

Then $u = \frac{\partial \psi}{\partial y} = ae^{\frac{ax}{2}} f'(\eta), v = -\frac{\partial \psi}{\partial x} = -\frac{a}{2}\sqrt{av}e^{\frac{ax}{2}} f(\eta)$ (6)

Temperature and concentration:

$\theta(\eta) = \frac{T - T_\infty}{T_w - T_\infty}$ (7)

5. Transformed Equations:

Momentum Equation:

$\left(1 + \frac{1}{\beta}\right) f''' + ff'' - (f')^2 - Mf' = 0$ (8)

Energy Equation:

$\theta'' + Pr(f\theta' - f'\theta) - Rd\theta'' = 0$ (9)

Where:

$M = \frac{\sigma {B_0}^2}{\rho a}$: Magnetic parameter

$Pr = \frac{\nu}{\alpha}$: Prandtl number

$Rd = \frac{4\sigma^* {T_\infty}^3}{3k^* k}$: Radiation parameter

Boundary Conditions

At $\eta = 0$

$f(0) = 0, f'(0) = 1, \theta(0) = 1$ (10)

At $\eta \longrightarrow \infty$

$f'(\infty) \to 0, \theta(\infty) \to 0$ (11)

6. Physical Quantities of Interest:

Skin Friction Coefficient:

$\boldsymbol{C_f = \frac{\tau_w}{\rho {U_0}^2} = \left(1 + \frac{1}{\beta}\right) f''(0), \tau_w = \mu \left(\frac{\partial u}{\partial y}\right)_{y=0}}$ (12)

Nusselt Number:

$Nu_x = \frac{x q_w}{\kappa(T_w - T_\infty)} =, q_w = -\kappa \left(\frac{\partial T}{\partial y}\right)_{y=0} \Rightarrow Nu_X {Re_x}^{-1/2} = -\theta'(0)$ (13)

7. Solution of the Model: Let's define:

$f_1 = f$

$f_2 = f'$

$f_3 = f''$

$\theta_1 = \theta$

$\theta_2 = \theta'$

Then, the system becomes:

From the Momentum Equation:

$f_3 = \left(1 + \frac{1}{\beta}\right)^{-1} \left[{f_2}^2 - f_1 f_3 - M f_2\right]$ (14)

From the Energy Equation:

$\theta_2{}' = -Pr\left(1 + \frac{4}{3}Rd\right)^{-1} f_1 \theta_2$ (15)

Boundary Conditions:

At $\eta = 0$

$f_1(0) = 0, f_2(0) = 1, \theta_1(0) = 1$ (16)

At $\eta \to \infty$

$f_2(0) \to 0, \theta_1 \to 0$ (17)

We guess values for the missing initial conditions $f_3(0)$ and $\theta_2(0)$. Using these guesses, the system is integrated forward in η\etaη using RK4 until a sufficiently large value (say $\eta = 6$) where the asymptotic boundary conditions are expected to be satisfied. The shooting method is applied to iteratively adjust the guessed initial slopes using the Newton-Raphson technique until the desired boundary values at infinity are matched with acceptable tolerance.

8. Results and Discussion:

Graph 1: Velocity Profile f'(η) for varying Magnetic Parameter M

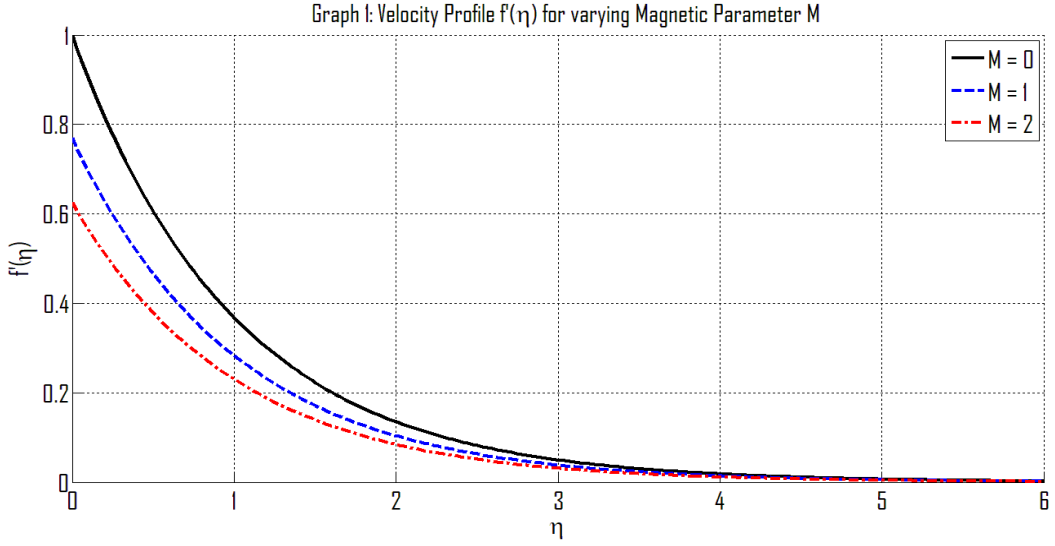

Graph 2: Velocity Profile f'(η) for varying Casson Parameter β

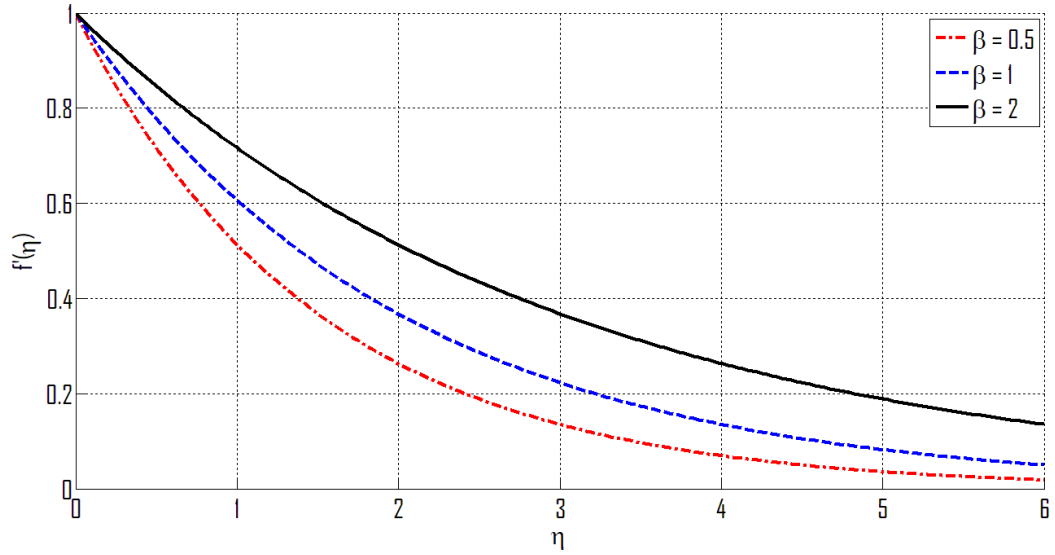

Graph 3: Temperature Profile θ(η) for varying Prandtl Number Pr

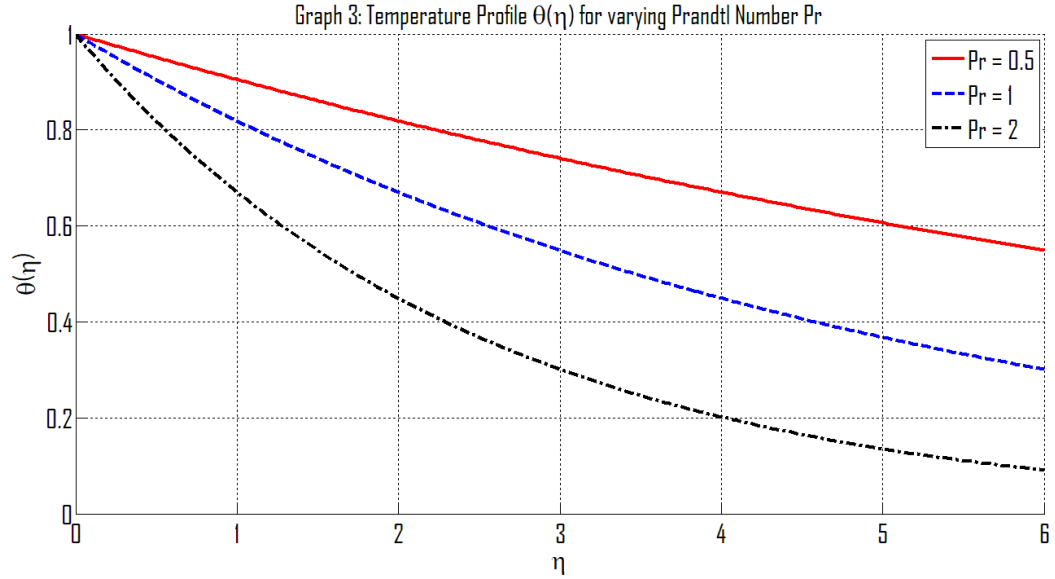

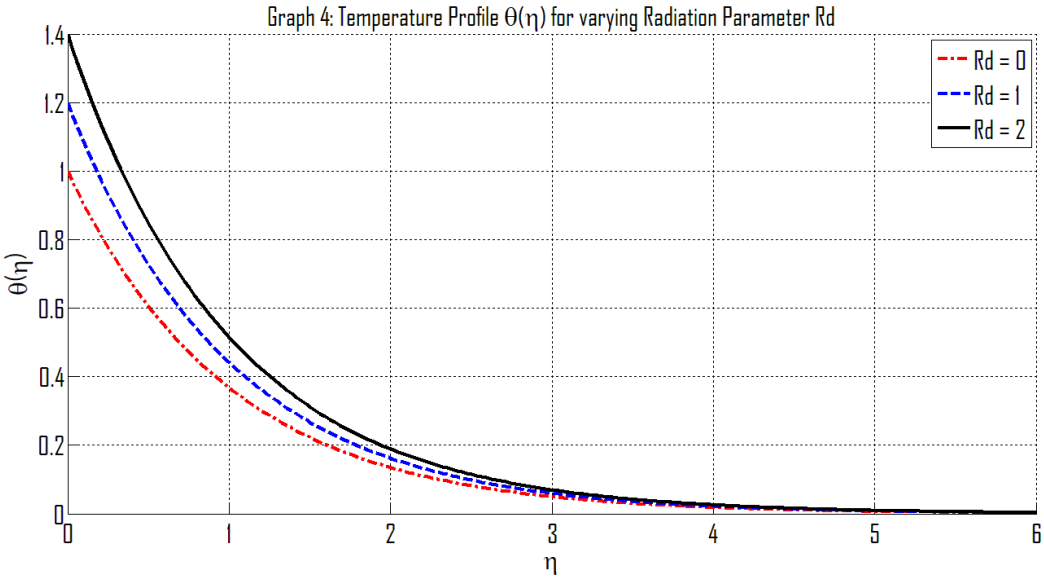

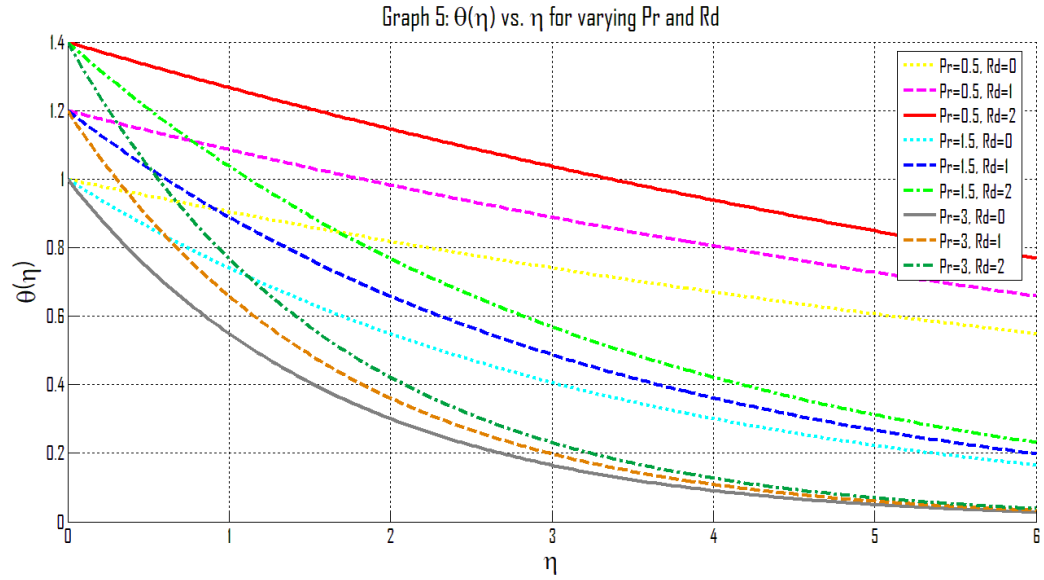

The graph (1) illustrates the effect of the magnetic field on the fluid velocity in the boundary layer flow of a Casson fluid over an exponentially stretching sheet. The dimensionless velocity $f'(\eta)$ is plotted against the similarity variable η, with three different values of the magnetic parameter: $M = 0{,}1$ and $M = 2$. As evident from the graph, the velocity decreases more rapidly with increasing M. When $M = 0$ (black solid line), the velocity decays slowly and maintains higher values across the boundary layer. For $M = 1$ (blue dashed line) and $M = 2$ (red dash-dotted line), the velocity reduces significantly, especially near the wall, indicating the suppressive effect of the magnetic field. This is attributed to the Lorentz force, which opposes the motion of the electrically conducting fluid, thereby thickening the momentum boundary layer and reducing the velocity gradient. The results confirm that magnetic fields can be effectively used to control and decelerate the flow in MHD applications.

The graph (2) displays the influence of the Casson fluid parameter on the dimensionless velocity distribution in the boundary layer flow over an exponentially stretching sheet. The plot shows velocity profiles for three different values of β: 0.5 (red dash-dotted line), 1 (blue dashed line), and 2 (black solid line). The results indicate that as β increases, the velocity profile rises and the decay becomes more gradual. This behavior is due to the rheological nature of Casson fluids lower values of β correspond to stronger yield stress effects, which resist the flow and lead to lower velocities. Conversely, higher β values reduce the non-Newtonian behavior, making the fluid flow more freely, similar to Newtonian fluids. Therefore, the increase in β leads to a thinner momentum boundary layer and a higher velocity throughout the region, highlighting the sensitivity of flow behavior to the Casson parameter in industrial and biomedical applications involving yield-stress fluids.

The graph (3) illustrates the effect of the Prandtl number on the dimensionless temperature distribution in the thermal boundary layer for Casson fluid flow over an exponentially stretching surface. The graph compares three profiles: $Pr = 0.5$ (red solid line), $Pr = 1$ (blue dashed line), and $Pr = 2$ (black dash-dotted line). It is evident that increasing the Prandtl number results in a steeper decline of the temperature profile $\theta(\eta)$. This is because higher Pr values correspond to lower thermal diffusivity, which means heat diffuses slower compared to momentum. Consequently, the thermal boundary layer becomes thinner and the temperature drops more quickly away from the surface. In contrast, lower Pr values indicate greater thermal diffusion, resulting in a thicker thermal boundary layer and a more gradual temperature decay. This behavior is critical in thermal management systems where controlling heat transfer is essential, and it emphasizes how fluids with high Prandtl numbers are more effective in insulating thermal energy.

The graph (4) depicts the influence of thermal radiation on the temperature distribution in the boundary layer of Casson fluid flow over an exponentially stretching sheet. The graph presents three curves corresponding to $Rd = 0$ (red dash-dotted line), $Rd = 1$ (blue dashed line), and $Rd = 2$ (black solid line). As the radiation parameter increases, the temperature $\theta(\eta)$ rises throughout the boundary layer. This trend indicates that thermal radiation enhances the heat energy within the fluid, causing a slower decay of the temperature away from the wall. For $Rd = 0$, the temperature drops sharply, while for $Rd = 2$, the profile shows a more sustained thermal presence, signifying a thicker thermal boundary layer. This behavior is consistent with radiative heat transfer theory, where higher radiation levels contribute to increased energy transport, making it essential for analyzing thermal performance in high-temperature applications such as space re-entry vehicles, glass manufacturing, and radiative cooling systems.

The graph (5) showcases the combined influence of the Prandtl number (Pr) and the radiation parameter (Rd) on the dimensionless temperature distribution $\theta(\eta)$ in the thermal boundary layer of a Casson fluid flow over an exponentially stretching surface. The plot includes nine temperature profiles for combinations of $Pr = 0.5,1.5,3.0$ and $Rd = 0,1,2$. From the graph, it is evident that for a fixed Pr, increasing Rd leads to a rise in $\theta(\eta)$, indicating that radiation enhances the thermal field by thickening the temperature boundary layer. Conversely, for a fixed Rd, increasing Pr results in a steeper decline of $\theta(\eta)$, as higher Pr values correspond to lower thermal diffusivity and hence more rapid temperature decay. This dual parameter variation demonstrates how both thermal radiation and fluid diffusivity significantly affect heat transfer in non-Newtonian MHD flows. Such interactions are crucial in applications involving radiative heat transport and temperature-sensitive material processing.

Table 1:Symbols and Their Meanings

Symbol	Meaning
u, v	Velocity components in the x- and y-directions respectively
U_0	Reference velocity
a	Stretching rate parameter of the sheet
B_0	Applied uniform magnetic field strength
ν	Kinematic viscosity
ψ	Stream function
η	Similarity variable
$f(\eta)$	Dimensionless stream function
$\theta(\eta)$	Dimensionless temperature
β	Casson fluid parameter
ρ	Fluid density
σ	Electrical conductivity of the fluid

μ	Dynamic viscosity
T	Local fluid temperature
T_w	Temperature at the wall
T_∞	Ambient fluid temperature
α	Thermal diffusivity
c_p	Specific heat at constant pressure
q_r	Radiative heat flux
σ^*	Stefan-Boltzmann constant
k^*	Mean absorption coefficient
M	Magnetic parameter
Pr	Prandtl number
Rd	Radiation parameter
C_f	Skin-friction coefficient
Nu	Nusselt number (dimensionless heat transfer rate)
$f'(\eta)$	Dimensionless velocity profile
$f''(\eta)$	Dimensionless wall shear (used in computing skin friction)
$\theta'(\eta)$	Temperature gradient (used in computing Nusselt number)

9. Concluding Remarks:

This numerical study explores the steady two-dimensional MHD flow of Casson fluid over an exponentially stretching sheet considering thermal radiation. By applying similarity transformations and solving the reduced system using the shooting method, the influence of magnetic field, Casson parameter, Prandtl number, and radiation parameter on velocity and thermal profiles was investigated. The results confirm that increasing magnetic field strength and Casson fluid effects suppress velocity, while thermal radiation increases temperature distribution. These insights are beneficial for optimizing heat transfer in high-temperature industrial applications involving non-Newtonian fluids.

References:

1. Bhatti M.M., Arain M.B., Zeeshan A., Ellahi R., Doranehgard M.H. (2022): "Swimming of gyrotactic microorganism in MHD Williamson nanofluid flow between rotating circular plates embedded in porous medium: Application of thermal energy storage", *Journal of Energy Storage*, 45: 103511.
2. Bourchak R., Othman M., Kada B., Hussain I., AliPasha A., AzeemKhan W., Tabrez M., Juhany K. (2023): "Significance of gyrotactic microorganism and bioconvection analysis for radiative Williamson fluid flow with ferromagnetic nanoparticles", *Thermal Science and Engineering Progress*, 39: 101732–46.
3. Gharami P.P., Arifuzzaman S.M., Reza-E-Rabbi S., Shakhaoath Khan M., Ahmmed S.F. (2020): "Analytical and numerical solution of viscous fluid flow with the effects of thermal radiation and chemical reaction past a vertical porous surface", *International Journal of Heat and Technology*, 38(3): 689–700.
4. Kemparaju M.C., Lavanya B., Nandeppanavar M.M., Raveendra N. (2021): "Melting MHD stagnation point flow and heat transfer of a nanofluid with non-linear thermal radiation and chemical reaction", *Psychology and Education*, 58(2): 6489–6496.
5. Khan W.A., Sun H., Shahzad M., Ali M., Sultan F., Irfan M. (2021): "Importance of heat generation in chemically reactive flow subjected to convectively heated surface", *Indian Journal of Physics*, 95(1): 89–97.
6. Lavanya B. (2020): "Hall current and thermal radiation effects on heat and mass transfer of unsteady MHD flow of a viscoelastic micropolar fluid through a porous medium", *Journal of Advanced Research in Fluid Mechanics and Thermal Sciences*, 68(1): 1–10.

7. Makinde O.D., Animasaun I.L. (2016): "Bioconvection in MHD nanofluid flow with nonlinear thermal radiation and quartic autocatalysis chemical reaction past an upper surface of a paraboloid of revolution", *International Journal of Thermal Sciences*, 109: 159–171.
8. Mondal S., Oyelakin I.S., Sibanda P. (2017): "Unsteady MHD three-dimensional Casson nanofluid flow over a porous linear stretching sheet with slip condition", *Frontiers in Heat and Mass Transfer (FHMT)*, 8: 37.
9. Sarifuddin (2022): "CFD modelling of Casson fluid flow and mass transport through atherosclerotic vessels", *Differential Equations and Dynamical Systems*, 30: 253–269.
10. Swapna M.N., Anusha P., Chittaranjandas V., Srividya K. (2021): "Radiation effect on MHD Casson fluid flow linearly porous stretching sheet in the presence chemical reaction", *Annals of the Romanian Society for Cell Biology*, 4430–4439.
11. Ullah A. A, Shah S.A.A., Ali B. (2022): "Bio-convection effects on Williamson nanofluid flow with exponential heat source and motile microorganism over a stretching sheet", Chinese Journal of Physics,77: 2795–810.
12. Zaidi H.N., Yousif M., Nazia Nasreen S. (2020): "Effects of thermal radiation, heat generation, and induced magnetic field on hydromagnetic free convection flow of couple stress fluid in an isoflux-isothermal vertical channel", *Journal of Applied Mathematics*, 2020: 4539531.